Model-Based Analysis and Design of a Microchannel Reactor for Tissue Engineering

Khamir Mehta, Jennifer J. Linderman

Department of Chemical Engineering, H.H. Dow Building, 2300 Hayward St., University of Michigan, Ann Arbor, Michigan 48109-2136; telephone: (734) 763-0679; fax: (734) 763-0459; e-mail: linderma@umich.edu

Received 23 August 2005; accepted 28 December 2005

Published online 3 April 2006 in Wiley InterScience (www.interscience.wiley.com). DOI: 10.1002/bit.20857

Abstract: Recently developed perfusion micro-bioreactors offer the promise of more physiologic in vitro systems for tissue engineering. Successful application of such bioreactors will require a method to characterize the bioreactor environment required to elicit desired cell function. We present a mathematical model to describe nutrient/growth factor transport and cell growth inside a microchannel bioreactor. Using the model, we first show that the nature of spatial gradients in nutrient concentration can be controlled by both design and operating conditions and are a strong function of cell uptake rates. Next, we extend our model to investigate the spatial distributions of cell-secreted soluble autocrine/paracrine growth factors in the bioreactor. We show that the convective transport associated with the continuous cell culture and possible media recirculation can significantly alter the concentration distribution of the soluble signaling molecules as compared to static culture experiments and hence needs special attention when adapting static culture protocols for the bioreactor. Further, using an unsteady state model, we find that spatial gradients in nutrient/growth factor concentrations can bring about spatial variations in the cell density distribution inside the bioreactor, which can result in lowered working volume of the bioreactor. Finally, we show that the nutrient and spatial limitations can dramatically affect the composition of a co-cultured cell population. Our results are significant for the development, design, and optimization of novel micro-channel systems for tissue engineering.

Keywords: mathematical modeling; bioreactor; transport; autocrine; tissue engineering; media recirculation

INTRODUCTION

Continuous cell culture protocols offer the promise of sufficient nutrient supply along with continuous waste removal and hence are often preferred for culturing cells to higher density or for developing tissue/organs in vitro. Perfusion systems are an important class of continuous culture systems and are widely used to culture cells for tissue engineering. Microchannel bioreactors have been developed to overcome the difficulty associated with design and operation of large complex perfusion systems and to have a larger and physiologically relevant surface to volume ratio. Advances in micro and nanofabrication techniques have enabled the development of novel designs of microchannel bioreactors to culture cells for tissue engineering (Andersson and van den Berg, 2004). Micro-scale perfusion systems have been reported for long term culture of hepatocytes, hematopoietic cells, fibroblasts, muscle cell lines, and osteoblasts (Allen et al., 2005; Gu et al., 2004; Horner et al., 1998; Koller et al., 1993; Leclerc et al., 2004, 2006). Most of the present approaches to develop such micro-scale systems for cell culture rely on many experiments to optimize the bioreactor operation and cell culture protocol. An important research topic in this field hence relates to the ability to reproducibly control the cell behavior inside the bioreactor by affecting the system design and operating variables.

A cell's behavior is governed in part by the microenvironment within which the cell resides. Apart from the usual physicochemical parameters such as pH, temperature, nutrient concentration, and mechanical stimuli, the bioreactor environment is also regulated by the collection of cells residing in it through a complex network of cell-secreted paracrine and autocrine soluble signals. For example, the epidermal growth factor-receptor system in epithelial cells and fibroblasts plays a significant role in cell expansion (Lauffenburger and Cozens, 1989) and the bone morphogenetic protein signaling system is important in mesenchymal stem cell and chondrocyte differentiation (Locker et al., 2004; Rawadi et al., 2003). A key factor to successful and reproducible operation of microchannel bioreactors for clinical or fundamental studies hence involves characterization of the microenvironment of the bioreactor.

Mathematical transport models can be used to understand the relationships between bioreactor design and operating variables and the microenvironment inside the bioreactor and to reduce expensive and time-consuming experimentation. In

Correspondence to: Jennifer J. Linderman
Contract grant sponsors: US Army Research Laboratories; Research Office grant
Contract grant number: DAAD 19-03-1-0168

particular, mathematical models hold promise for defining operating windows, hypothesis testing, data interpretation, and optimization of these reactors. Transport in perfusion bioreactors has been studied in various contexts and mathematical transport models at various levels of complexity have been developed to characterize the microenvironment for a wide variety of bioreactor designs (Botchwey et al., 2003; Galban and Locke, 1999; Ghanem and Shuler, 2000; Horner et al., 1998; Netti and Jain, 2003; Williams et al., 2002). Transport of nutrients such as oxygen has been extensively studied for various reactor geometry and cell types (Allen and Bhatia, 2003; Horner et al., 1998; Obradovic et al., 2000; Pathi et al., 2005; Roy et al., 2001).

Here, we build on the excellent background of the available models and develop a generic model-based design framework for a perfusion-microchannel bioreactor. We begin by presenting a coupled nutrient transport and cell proliferation model and analyze the model for various scenarios inside a rectangular channel bioreactor. We present the results of the steady state nutrient transport model with constant cell density and interpret them to better understand the nature and existence of spatial gradients of nutrients and cell-secreted autocrine/paracrine molecules inside the bioreactor. We also consider these gradients when recirculation of used media is incorporated. Next, we study the impact of the nutrient gradients on the evolution of the cell population inside the bioreactor. Finally, we also investigate the implication of nutrient and spatial limitations on the sustained viability and proliferation of a heterogeneous population of cells.

METHODS

Model Formulation

The spatial and temporal changes in the concentrations of various species of interest (nutrients, metabolites, soluble exogenous, and endogenous growth factors) inside the bioreactor can be modeled using the reaction diffusion equation. The general mass balance equation of soluble component i in the microenvironment of the bioreactor in terms of concentration of soluble species (c_i) in the media takes the form

$$\frac{\partial c_i}{\partial t} + u \cdot \nabla c_i = \nabla \cdot (D_{ei} \nabla c_i) + R_{i,net} \qquad (1)$$

where D_{ei} is the effective diffusivity of species i, u is the velocity profile of media inside the bioreactor, and $R_{i,net}$ represents the net volumetric uptake, secretion and degradation rate for the species i and is dependent on the cell population density.

Concentrations of nutrients can affect cell population dynamics and cell population density in turn can affect the distribution of nutrients. Quantitative models of cell behavior are, therefore, coupled to the nutrient transport models. Furthermore, cell proliferation and differentiation behavior is known to be affected by concentration levels of growth factors in various cell types including hematopoietic cells and stem cells (e.g., Zandstra et al., 1997). In such cases, information on the spatial distribution of growth factors as given by the transport model can help to identify the differentiation patterns in the bioreactor. We consider the case of cell proliferation inside the bioreactor and use the following continuous cell growth model to describe the dynamics of the proliferating cell population in terms of cell density of cell type j (ϕ_j)

$$\frac{\partial \phi_j}{\partial t} = \mu_{g,j} \phi_j - k_d \phi_j \qquad (2)$$

Here $\mu_{g,j}$ represents the specific growth rate of cell type j and k_d represents the death rate constant. The growth rate $\mu_{g,j}$ is a function of the nutrient concentration(s) and also the cell density (e.g., logistic dependence), making equation (2) non-linear. We refrain from using a complex cell death/loss model that includes, for example, the effects of toxic substances or shear stress at the cell surface or flow-induced cell wash out so that we can focus on the general design rules coming from our model analysis. Furthermore, we know that the operating flows fixed based on avoiding cell wash out would be at low Reynolds number (Re $\sim$0.001, Leclerc et al., 2006) leading to lower shear stresses. However, for application to a particular problem, such analysis might be important to add.

Equation (2) is dependent on the spatial dimensions through the nutrient concentration dependence of the cell growth rate. The model accounts for heterogeneous coexisting cell populations and also for the competition for space and nutrients among them. The model in the present form does not account for transition of cell type j to any other cell type through differentiation or maturation; however, the formulation does permit the incorporation of continuous kinetics-based models of cell differentiation (e.g., da Silva et al., 2003, for hematopoietic stem cell differentiation) for a more complete evaluation of the bioreactor performance in advanced tissue engineering applications. Also, in the current study we limit our model to non-motile cells, though one could include terms in the cell balance equations to account for cell migration (Lauffenburger and Linderman, 1993).

In principle the solution of equations (1)–(2) can be obtained numerically for any $R_{i,net}$, $\mu_{g,j}$, and k_d and any reactor geometry. The flow profile u can be obtained by using information on geometry and solving the relevant fluid dynamics equations. However, information on the system can help us make some vital simplifications in the model equations and hence make the solution process more manageable. For the current work, we solve the model for the simple case of rectangular microchannel reactor geometry as per Figure 1, which shows the schematic of a rectangular microchannel fabricated in PDMS (poly dimethyl siloxane) using soft lithography technology or in polycarbonate substrate by polymer micromachining. The media flows inside the channel using a pumping device from a reservoir whose volume is usually much larger than the channel volume (not shown). Although the current study is restricted

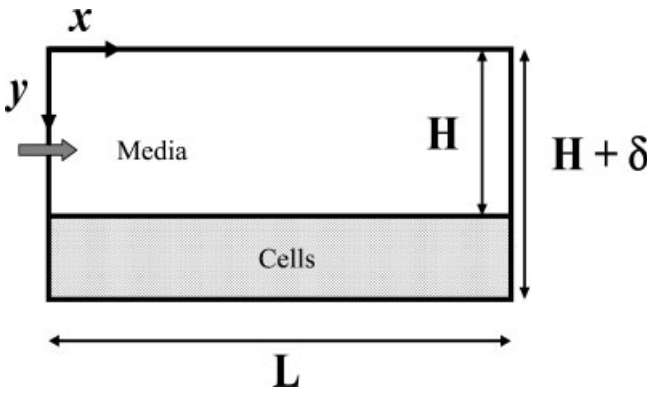

Figure 1. Schematic representation of rectangular microchannel bioreactor geometry model (side view). The media flows in the x direction and the cell population is assumed to be selectively located at the bottom of the channel (shown as shaded region) at y = H dividing the microchannel into two domains: the flow domain and the cell domain. Usually for monolayer cultures $\delta << H$, and the width of the channel (W) is large enough so that the model can be analyzed in two dimensions.

to the geometry shown in Figure 1, the simplification should hold for most microchannel bioreactors culturing adherent cells, with no or minimal modifications. Also, it should be noted that the model formulation and the subsequent development and coupling of the transport equations with the cellular proliferation dynamics described here is general and can be extended to other reactor geometries and co-ordinate systems.

We first consider a once through media flow without recirculation. We can simplify the model for the rectangular microchannel based on the channel dimensions which usually ensure that we can neglect the changes along the width (W), (W $\gg$ H) and hence analyze the problem in 2-D. Mammalian cells are likely to be adherent and found at the bottom of the channel either by themselves or encapsulated in polymeric carriers. Thus the channel is divided into two domains. In the top domain, there are no cells; nutrients are transferred to the bottom cell domain by diffusion. We hence hypothesize a geometry where the cell domain of relatively small thickness δ is adjacent to the unidirectional flow domain. With this assumption, the mass balance equation (1) in the flow domain is coupled to the cellular uptake/secretion through a boundary condition at the interface and the volumetric uptake rate (R_i) vanishes. Further, we neglect the diffusion in the axial direction compared to the convective flux and the volumetric degradation to arrive at the following simplified equation for species conservation in the flow domain:

$$\frac{\partial c_i}{\partial t} + u_x \frac{\partial c_i}{\partial x} = D_{ei} \frac{\partial^2 c_i}{\partial y^2} \tag{3}$$

The flow profile in the reactor shown in Figure 1 can be solved explicitly using the Navier-Stokes equation with the incompressible assumption using a computational fluid dynamics approach. However, for the current work, considering the small conduit volume, it is sufficient to assume a laminar flow profile in the flow domain. We assume a unidirectional flow in the axial direction and use the steady state velocity profile for pressure driven flow between two plates for low Reynolds number given by

$$u_x(y) = 6\langle u \rangle \frac{y}{H}\left(1 - \frac{y}{H}\right) \tag{4}$$

where $< u >$ is the average velocity and H is the height of the flow domain, which is approximately equal to the height of the microchannel for a cell mono-layer ($\delta << H$).

The general initial (equations (5) and (6)) and boundary conditions (equations (7)–(9)) for the set of equations (2)–(4)) are

$$c_i(x, y, 0) = 0 \tag{5}$$

$$\phi_j(0) = \phi_{j0} \tag{6}$$

$$-D_{e,i} \frac{\partial c_i}{\partial y}(x, 0, t) = F_{U,i} \tag{7}$$

$$-D_{e,i} \frac{\partial c_i}{\partial y}(x, H, t) = F_{L,i} \tag{8}$$

$$c_i(0, y, t) = c_{in} \tag{9}$$

where ϕ_{j0} denotes the initial (cell seeding) density of cell type j. The flux boundary condition at the upper surface of the media flow layer (F_U) is determined by the permeability of the material in which the microchannel is etched out. PDMS, the material of interest here, can allow significant fluxes of gases across into the media due to its high permeability, while diffusivity of gases in polycarbonate is not significant. For specific consideration of gaseous components like oxygen, we use a mass transfer co-efficient ($k_{l,a}$) to characterize the diffusion of gaseous nutrients from the PDMS layer, where c_i^{sat} is related to the solubility of component i in PDMS

$$F_{U,i} = k_{l,a}(c_i^{sat} - c_i) \tag{10}$$

For other nutrients and growth factors we assume F_U is negligible. The flux boundary condition at the lower surface (equation (8)) of the flow layer (F_L) is determined by the uptake rate of cells and the cell density, and hence is coupled with the cell population balance equation. The axial boundary condition at the inlet is the Dirichlet type (equation (9)), with specified concentration.

Recirculation of media in the bioreactor offers the promise to retain the cell-secreted growth factors, and can be achieved in two possible manners as shown in Figure 2. In either case, we need to modify the boundary condition at the reactor inlet (equation (9)) to account for the recirculation, which can be

DOI 10.1002/bit

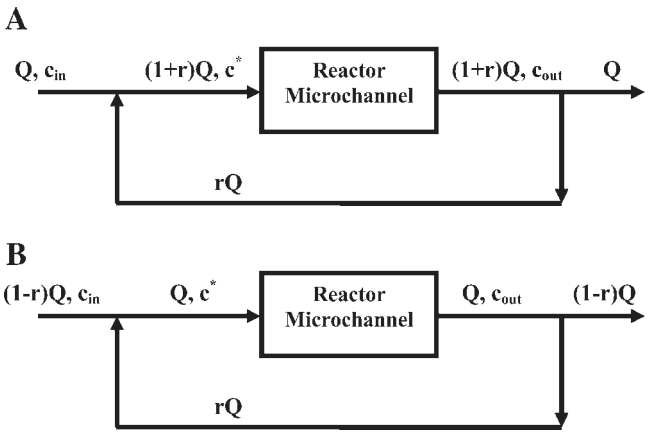

Figure 2. Two possible schemes for recirculation. Q denotes the volumetric flow rate, c denotes the concentration, and r is the recirculation ratio defined as per the figure. In scheme (**A**) the inlet flow rate is kept constant, so that the flow inside the channel is changed when the recycle fraction is changed, while in scheme (**B**), the flow across the microchannel is kept constant and the inlet flow is adjusted based on the recycle fraction.

done by using mass balance equations for the recycle loop. For example in case of scheme B for constant inlet velocity, defining the recirculation ratio r as the fraction of the outlet flow which is recycled back, the inlet concentration (c^*) can be calculated from the media concentration (c_{in}) and the reactor outlet concentration (c_{out}) for species i

$$c_{\text{i}}^{*} = (1-r)c_{\text{i,in}} + rc_{\text{i,out}} \tag{11}$$

Constitutive Relationships for Uptake/Secretion and Cell Proliferation Rates

The chemical species under consideration could be essential growth factors, nutrients, or the products of cell metabolic activities. Most nutrient or metabolite uptake rates are known to follow saturation kinetics and are modeled with Michaelis-Menten (MM) kinetics (Allen and Bhatia, 2003; Ben-Abraham et al., 2003; Obradovic et al., 2000), and the values of the MM parameters can be measured from experiments done with static culture protocols. The mathematical expression of the specific uptake rate for species i by cell type j ($R_{\text{up,ij}}$) would thus take the form

$$R_{\text{up,ij}} = \left(\frac{V_{\text{max,ij}}c_{\text{i}}}{K_{\text{m,ij}} + c_{\text{i}}}\right) \tag{12}$$

$V_{\text{max,ij}}$ and $K_{\text{m,ij}}$ are the MM parameters. The actual uptake rate depends on the specific uptake rate and the local cell density and it can be assumed that the actual uptake rate is directly proportional to the cell density (Jorjani and Ozturk, 1999). The corresponding flux boundary condition at the cell-media interface for a general case with N cell types hence would be

$$\text{F}_{\text{L,i}} = \sum_{\text{j}=1}^{N} R_{\text{up,ij}}\phi_{\text{j}} = \sum_{\text{j}=1}^{N}\left(\frac{V_{\text{max,ij}}c_{\text{i}}}{K_{\text{m,ij}} + c_{\text{i}}}\right)\phi_{\text{j}} \tag{13}$$

The model in its present form can also be extended for cell-secreted molecules, for example growth factors and other chemical signaling molecules, which may act in an autocrine or paracrine manner and play an important role in governing cell viability and function. The mathematical modeling of autocrine growth factor secretion and their regulation has been studied using various mathematical approaches to understand the associated signaling pathways (Bhalla and Iyengar, 1999; Shvartsman et al., 2001), particularly for the EGF system (Wiley et al., 2003). However, for the present study we consider an autocrine growth factor affecting the cell growth rate, and consider the case where the secretion of the growth factor is constant for each cell (i.e, the secretion is not regulated), and is taken up by the cells in a dose-dependent manner described by MM kinetics. We use this simplistic set-up to understand the general guiding principles for bioreactor design and optimization, particularly for reactors with recirculation. For the case of a soluble growth factor described above, the flux conditions at the domain bottom ($\text{y} = H$) for homogenous population of a single cell type would be

$$\text{F}_{\text{L,gf}} = q_{\text{gf}}\phi - \left(\frac{V_{\text{max,gf}}c_{\text{gf}}}{K_{\text{m,gf}} + c_{\text{gf}}}\right)\phi \tag{14}$$

The subscripts on the cell density ϕ have been dropped as we consider just a single cell type for this case. q_{gf} represents the specific secretion rate for autocrine growth factor while $V_{\text{max,gf}}$ and $K_{\text{m,gf}}$ are uptake parameters. Important simplifying assumptions in the above model for cell-secreted soluble growth factor are that within the cell domain the uptake of the species is spontaneous and without any further diffusive resistance and that the secretion rate (q_{gf}) is constant.

We use a logistic cell growth model with substrate inhibition kinetics for growth rate dependency on nutrient concentration (Pathi et al., 2005). The later is chosen to reflect the impact of nutrients like oxygen on cell growth as it is known that conditions with high concentration of oxygen can be detrimental for cell growth, while lower concentrations can decrease the growth rate. The general expression for cell growth for cell type j, assuming limiting nutrient species i, hence can be taken as:

$$\mu_{\text{g,j}} = \mu_{\max}\left(1 - \frac{\sum_{\text{j}}\phi_{\text{j}}}{\phi_{\max}}\right)\prod_{i}\left(\frac{k_{1\text{ij}}c_{\text{i}}}{1 + k_{2\text{ij}}c_{\text{i}} + k_{3_{\text{ij}}}c_2^{\text{j}}}\right) \tag{15}$$

where, $\phi_{\max}$ is the maximum cell density or carrying capacity of the system, and c_{i} represents the concentration of limiting nutrient species. The growth model parameters $k_{1,\text{ij}}$ $k_{2,ij}$ and $k_{3,\text{ij}}$ represent the impact of concentration of nutrient species i on the growth of cell type j. A value of parameter $k_{3,\text{ij}}$ close to zero indicates the standard Monod type kinetics, while a larger value indicates a detrimental effect of the nutrient on cell growth at higher concentrations. The summation is carried over all the cell types, and the product is over all the limiting nutrient/growth factor species.

Table I. Model non-dimensionalization scheme and dimensionless variables/groups.

Dimensional variable/parameter	Description	Dimensionless variable/parameter	Definition
c	Concentration	C	$C = c/c_{in}$ or $C = c/K_m$
x	Axial distance	X	$X = x/L$
y	Height dimension	Y	$Y = y/H$
u_x	Velocity	U	$U = u_x/< u >$
t	Time	τ	$\tau = t/t_d$
ϕ	Cell density	Φ	$\Phi = \phi/\phi_0$
k_1	Cell growth model parameter	K_1	$K_1 = k_1 * c_{in}$
k_2	Cell growth model parameter	K_2	$K_2 = k_2 * c_{in}$
k_3	Cell growth model parameter	K_3	$K_3 = k_3 * (c_{in})^2$

Dimensionless groups	Description	Definition
α	Geometric ratio	$\alpha = L/H$
Pe	Peclet number	$Pe = < u > H/D_e$
Da	Damkohler number	$Da = V_{max}\phi H/(D_e c_{in})$ (Nutrient) or $Da_{up} = V_{max}\phi H/(D_e K_m)$ (growth factor, uptake) or $Da_{in} = q\phi H/(D_e K_m)$ (growth factor, secretion)
Sh	Sherwood number	$Sh = k_{l,a}H/D_e$
γ	Ratio of influx to uptake of growth factor	$\gamma = Da_{in}/Da_{up} = q/V_{max}$
λ	Ratio of time scales	$\lambda = L/(t_d < u >)$

Solution to Model Equations

We solve the system of equations (2)–(9) in a non-dimensional framework as a convenient way to explore the large number of parameters in a systematic manner. Table I gives the non-dimensionalization scheme for variables and the key dimensionless groups involved. The model equations in working/non-dimensional form for the general case as well as the specific cases described below are tabulated in Table II.

The partial differential equation (1) or (3)) governing the nutrient/growth factor distribution can be decoupled from the cell proliferation dynamics equation (2) by assuming constant cell density to give results which are valid for short times. Further, the model equations can be solved at steady state to arrive at the steady state spatial distribution of nutrient and/or growth factor inside the reactor for a given cell population density. Solving the fully coupled unsteady state model in its full form (equations (2)–(9)) is computationally expensive, as the time step required to solve the species conservation equation is much smaller than that required by the cell proliferation equation. The cell proliferation time scale characterized by the doubling time (t_d) is of the order of hours while the residence time (t_r) of the media inside the reactor is of the order of minutes ($t_r = L/< u >$). However, this knowledge leads to a useful approximation of the model equations where we can assume that while considering the dynamics of cell proliferation, the concentration field is always at the steady state. This pseudo steady state analysis is valid for small values of λ (defined as the ratio of two time scales, $\lambda = t_r/t_d = L/(t_d < u >)$) and enables us to solve the cell population balance equation in its unsteady form, while the species conservation equation can be solved at steady state. We use these results to analyze the effect of nutrient gradients on cell density distribution and vice-versa.

The dimensionless analysis broadens the applicability of the model results and undermines the need to get the actual parameter values for the present study. Nevertheless, the model parameters for simulation are chosen to reflect literature data whenever available. We use the published data for reactor geometry and oxygen consumption of hepatocytes (Allen and Bhatia, 2003; Roy et al., 2001) for our calculations. Further, the oxygen uptake is reported to vary up to 2 orders of magnitude for wide variety of cell types (Guarino et al., 2004) and hence we vary the parameter Da to simulate different cell types. Similarly, the uptake of the cell-secreted autocrine factor is varied based on estimation of the range of autocrine ligand secretion rates as reported earlier (Oehrtman et al., 1998). The base case values of the parameters as estimated from literature cited above are tabulated in Table III.

Model equations in non-dimensional form (Table II) were solved numerically using finite element software FEMLAB (v. 3, Consol AB Inc) for a representative set of parameters (Table III). We study the effect of recirculation by simultaneously solving the species balance partial differential equations (equations (3)–(9)) and the mass balance equations in the recycle loop (equation (10)) in an iterative manner. Analytical solutions for the given set of equations can be found for a uniform velocity profile and zero order oxygen flux and constant cell density, and these were compared to the numerical solutions to confirm the sanctity of the numerical solution procedure.[1]

[1]Furthermore, steady state model results for the case of constant cell density and without recirculation (case (b) of Table II, with $Sh = 0$, $Da = 0.17$, and $Pe/\alpha = 0.19$) were compared and were found to be in agreement with the published numerical solutions for the outlet concentration of oxygen in a flat bed culture of rat hepatocytes (Allen and Bhatia, 2003).

DOI 10.1002/bit

Table II. Dimensionless model equations.

#	Case	Working/dimensionless equations	Initial and boundary conditions
a	General case	$\lambda\frac{\partial C_i}{\partial \tau}+U\frac{\partial C_i}{\partial X}=\frac{\alpha}{Pe}\frac{\partial^2 C_i}{\partial Y^2}$ $\frac{\partial \Phi_j}{\partial \tau}=(t_d\mu_{g,j})\Phi_j-(k_d t_d)\Phi_j$	$C_i(X,Y,0)=0$ $C_i(0,Y,\tau)=C_{i,in}$ $\frac{\partial C_i}{\partial Y}(X,0,\tau)=Sh(C^{sat}-C)$ $\frac{\partial C_i}{\partial Y}(X,1,\tau)=Da\frac{C(X,1,\tau)\Phi(X,\tau)^*}{\left(\frac{K_m}{c^*}+C(x,1,\tau)\right)}$ $\Phi_j(X,0)=1$
b	Steady state with constant cell density (nutrient)	$U\frac{\partial C_i}{\partial X}=\frac{\alpha}{Pe}\frac{\partial^2 C_i}{\partial Y^2}$ $\Phi=1$	$C_i(0,Y,\tau)=1$ $\frac{\partial C_i}{\partial Y}(X,0,\tau)=0$ or for Gaseous nutrient $\frac{\partial C_i}{\partial Y}(X,0,\tau)=Sh(C^{sat}-C)$ $\frac{\partial C_i}{\partial Y}(X,1,\tau)=Da\frac{C(X,1,\tau)}{\left(\frac{K_m}{c_{in}}+C(x,1,\tau)\right)}$
c	Steady state with constant cell density (autocrine growth factor)	$U\frac{\partial C_i}{\partial X}=\frac{\alpha}{Pe}\frac{\partial^2 C_i}{\partial Y^2}$ $\Phi=1$	$C_i(0,Y,\tau)=0$ $\frac{\partial C_i}{\partial Y}(X,0,\tau)=0$ $\frac{\partial C_i}{\partial Y}(X,1,\tau)=Da\left[\frac{C(X,1,\tau)}{(1+C(x,1,\tau))}-\gamma\right]$
d	Pseudo steady state	$U\frac{\partial C_i}{\partial X}=\frac{\alpha}{Pe}\frac{\partial^2 C_i}{\partial Y^2}$ $\frac{\partial \Phi_j}{\partial \tau}=(t_d\mu_{g,j})\Phi_j-(k_d t_d)\Phi_j$	$C_i(0,Y,\tau)=C_{i,in}$ $\frac{\partial C_i}{\partial Y}(X,0,\tau)=0$ $\frac{\partial C_i}{\partial Y}(X,1,\tau)=Da\frac{C(X,1,\tau)}{\left(\frac{K_m}{c_{in}}+C(x,1,\tau)\right)}$ $\Phi(X,0)=1$
e	Spatial limitations only	$\frac{\partial \Phi_j}{\partial \tau}=(t_d\mu_{g,j})\Phi_j-(k_d t_d)\Phi_j$	$\Phi_j(X,0)=1$

*c^* is the concentration scaling variable. It is equal to the inlet concentration c_{in} for nutrients, and equal to MM parameter K_m for the autocrine growth factor.

RESULTS AND DISCUSSION

Steady State Model Analysis at Constant Cell Density: Nutrient Distribution

A good measure of the performance of the bioreactor is the ability of the bioreactor to sustain a cell population and provide it with the required nutrients to ensure desired cell function and viability. The depletion of nutrient from the media by cell uptake as it flows downstream of the reactor creates axial nutrient gradients at the cell-media interface which may not be desirable. Non-dimensionalization of the model equations (Table II) shows that two dimensionless groups are important in determining the concentration distribution of the species inside the bioreactor, Pe/α ($=<u>H^2/(D_eL)$) and the Damkohler number ($Da=V_{max}\,\phi\,H/D_e c_{in}$). The dimensionless group Pe signifies the Peclet number ($Pe=<u>H/D_e$), and it represents the ratio of convective transfer of species in the axial direction to the diffusive flux within the channel directed towards the lower end of the channel that is towards the cell domain. The Damkohler number is a measure of relative rates of the total cellular uptake and the diffusive flux from the bulk media. The value of Da is largely dependent on the cell type and its metabolic state and also on the cell density. For example here, the value of $Da=0.21$ for oxygen transport corresponds to the rat hepatocytes ($V_{max}=3.8\times10^{-16}$/molcell/s, Allen and Bhatia, 2003) cultured at a cell density of 2.1×10^9 cells/m^2.

We first simulate the condition of the reactor for a constant cell density. Figure 3 shows the effect of the parameters Pe/α and Da on the non dimensional outlet concentration (C_{out}) of

Table III. List of parameter values.

Parameter	Value	Units
General parameters		
L	5.5	cm
H	100	μm
W	2.8	cm
$< u >$	2.0×10^{-3}	m/s
ϕ_0	2.1×10^{9}	cells/m^2
Parameters for nutrient distribution simulation[a]		
V_{max}	3.8×10^{-16}	mol/s/cell
D_e	2.0×10^{-9}	m^2/s
c_{in}	0.19	mol/m^3
K_m	0.006975	mol/m^3
Parameters for autocrine factor distribution simulation[b]		
V_{max}	1.66×10^{-22}	mol/s/cell
Q	1.66×10^{-2}	mol/cell/s
D_e	1×10^{-10}	m^2/s
c_{in}	0	mol/m^3
K_m	1	μmol/m^3
Parameters for cell growth simulation[c]		
K_1	6	—
K_2	2	—
K_3	5	—
$(t_d \mu_{max})$	0.693	
$(t_d k_d)$	0.0693	
ϕ_{max}	4.2×10^{9}	cells/m^2
$\phi 0$	4.2×10^{8}	cells/m^2

[a]As per Allen and Bhatia (2003).
[b]Estimated values based on Oehrtman et al. (1998).
[c]The parameters for the cell proliferation model (K_1, K_2, K_3) were estimated roughly from the data on the doubling times of cells in media of different glucose/serum concentrations as reported by Guarino et al. (2004) and were chosen so as to have the maximum growth rate at dimensionless concentration value $C = 0.5$.

the nutrient species at the cell-media interface ($X = 1$, $Y = 1$). The outlet concentration is scaled to the inlet concentration, and hence the dimensionless concentration (C) of nutrient at the inlet is equal to unity, making $(1 - C_{out})$ the effective concentration drop or axial gradient inside the bioreactor. Diffusive gradients in the Y direction can also exist inside the reactor, especially for $Pe/\alpha > 1$ and $Da > 1$, as shown in the inset of Figure 3 and we hence consider the concentration at the cell-media interface, as it is indicative of the actual concentration in the cell micro-environment.

For a given cell density and cellular uptake rate (fixed Da), as we increase the parameter Pe/α, the convective flux dominates and the outlet concentration of the nutrient increases. The diffusive flux of nutrient across to the cell domain is also higher due to higher concentrations in the media domain (not shown). Increased convective flux signifies higher influx rates, and also the fact that nutrients are pushed through the reactor faster than they can diffuse and be consumed by the cells. We hence conclude that increasing flow rate or changing the operating parameters so as to selectively increase Pe/α can lead to decreasing the axial gradients inside the bioreactor. Further, for a given Pe/α, an increase in Da is reflective of the increased rates of consumption by cells, and hence a corresponding decrease in the outlet concentration or increased nutrient gradient is observed.

Further useful conclusions regarding the design and operation of the bioreactor can be drawn from Figure 3. Of the variables included in the two dimensionless groups, we can roughly classify the media flow rate and the inlet concentration of the nutrient ($< u >$ and c_{in}) as operational variables. For example, during the operation of the bioreactor, the media flow rate can be used for controlling the concentration gradients of the nutrient so that the concentration of a particular nutrient does not fall below a certain threshold value inside the reactor. However, the choice of the media flow rate is usually limited by the fact that cells cannot be subjected to high levels of flow associated shear stress, and hence the media flow rate can only be used as a fine control. Nevertheless, the graph clearly also gives the options of designing the reactor geometry variables (L, H) which can have similar effect on the concentration gradient. At the design stage, we can determine, from the graph, the design variables for culturing cells to a given cell density so that the concentration of the nutrient is always above a prescribed minimum value. Conversely, for a given reactor geometry and maximum flow rate (e.g., determined by the reactor limitations and shear stress considerations), the model results can be used to estimate the maximum value of the cell density the bioreactor can support by estimating the value of Da for the desired outlet concentration of nutrient, given the value of Pe/α. The results of Figure 3 can also be used to quickly answer non-trivial design questions. For example, the effect of length on the axial gradients is fairly intuitive, as increasing the length will increase the gradients by decreasing the parameter Pe/α, but the effect of channel height cannot be readily predicted. The group Pe/α has a quadratic dependence on the height, while the Da is directly proportional to height. Hence, increasing the height of the channel will increase Pe/α, shifting the operating point on the curve on Figure 3 towards the right, and increase Da, shifting the operating point down, but more to the right than down. Thus depending on the location of the original operating point, increase in height can decrease, increase or have negligible effect on the outlet concentration of the nutrient. For example, as per Figure 3, if we were to double the height when operating at a value of $Da = 1.05$, and Pe/α value less than 1, the new operating point will be shifted to the curve with $Da = 2.1$, and a Pe/α value of about 4, increasing the outlet concentration. If, however, the original operating point was close to $Pe/\alpha = 2$, we would see an effective decrease in the outlet concentration, or increased axial gradient. In general, the channel height can be used to adjust the nutrient distribution in the reactor and the effect of changing the height on the cell culture can give us useful insights on the operating point of the bioreactor.

In addition to delivery by media flow, oxygen can be supplied by surface aerators or membrane oxygenators (Roy et al., 2001). Microchannel reactors fabricated from PDMS are also recommended in literature (Leclerc et al., 2003) as

DOI 10.1002/bit

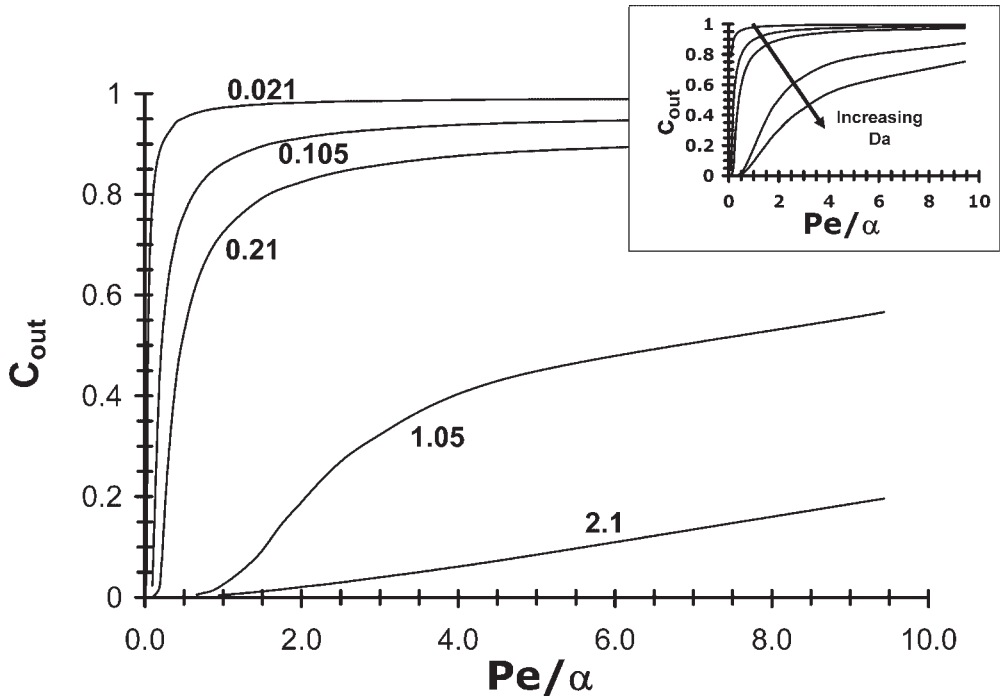

Figure 3. Steady state non dimensional exit concentration C_{out} at the cell-media interface (at X = 1, Y = 1) as a function of the non dimensional group Pe/α for constant cell density. The curves are shown for various values of Damkohler number (Da) shown in the figure. The base case parameter values (for Da = 0.21) are as per Table III. The concentration is scaled w.r.t the inlet concentration set at $c_{in} = 190$ μM and the Sherwood number is set equal to zero (Sh = 0). Inset shows the average concentration $C_{avg} = \frac{1}{H}(\int_0^H c dy)$ of the nutrient at the outlet for same parameter values. It can be seen that while the average concentration can differ from the concentration at the cell-media interface when Pe/α > 1 and Da > 1, the nature of the curves for both the cases is similar.

they support diffusion of oxygen due to their large gas permeability. We used our model to investigate the significance of gas diffusion as related to the design and operation of the bioreactor. Figure 4 shows the dimensionless outlet concentration of gaseous nutrient for the case of non-zero flux through the PDMS layer for $Da = 0.21$ and typical values of Sherwood numbers (Roy et al., 2001). The magnitude of diffusive flux is governed by the value of the Sherwood number (Sh), defined as the ratio of the diffusive transfer rate through the PDMS top surface to the diffusion rate in the media ($Sh = k_{l,a}H/D_e$). Our results indicate that the diffusive flux through the top surface is important for low values of Pe/α ($Pe/\alpha < 1$). Also at low Pe/α, significant axial gradients can exist in the reactor for lower values of Sh ($Sh < 0.5$), which is consistent with the observations of Roy et al. (2001). At higher values of Pe/α, convective flux dominates and diffusion through the top surface does not affect the concentration of the species at the cell interface. Significantly, then, the use of highly permeable material or external supply using membranes to deliver oxygen will not increase oxygen availability to cells in the reactor for $Pe/\alpha > 1$. Thus the model can be used to infer the optimal design to balance the nutrient delivery using flow and surface transfer and keep a desired level of nutrient inside the bioreactor.

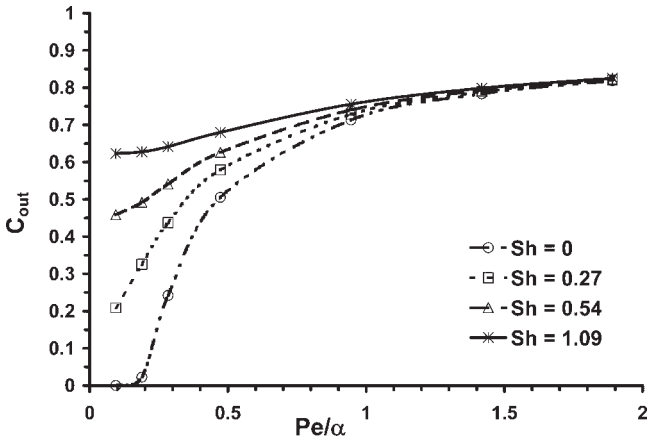

Figure 4. Steady state non dimensional exit concentration C_{out} of gaseous nutrients at the cell-media interface (at X = 1, Y = 1) as a function of the non dimensional group Pe/α for constant cell density and for non zero values of diffusive flux from the upper boundary. The curves are shown for various values of Sherwood number (Sh) shown in the figure. The base case parameter values are set at are as per Table III and set at Da = 0.21. The concentration is scaled w.r.t the inlet concentration set at $c_{in} = 190$ μM, and the dimensionless saturated concentration at the nutrient/media interface (C^{sat}) is set equal to unity.

Steady State Model Analysis at Constant Cell Density: Transport of Cell-Secreted Growth Factors

We illustrate the use of model analysis for soluble cell-secreted growth factors by considering a simple case of a single representative growth factor, which acts in an

autocrine manner in a homogeneous cell population. Non-dimensionalization of the model equations (Table II) gives two relevant Damkohler number groups: Da_{in} ($q_{gf}\,\phi\,H/(DK_m)$), associated with the influx of the soluble growth factor to the flow domain by the cells, and Da_{up} ($V_{max,gf}\,\phi\,H/(DK_m)$), associated with the uptake as described above. Both dimensionless groups represent the ratio of rates of secretion/uptake to the diffusive flux from the flow domain. Importantly, we define the parameter γ as the ratio of the influx to uptake Damkohler numbers ($\gamma = Da_{in}/Da_{up}$). Larger values of γ are indicative of ample secretion of the growth factor and therefore the growth factor receptors are most likely saturated and loss of growth factor due to convective transfer may not be important. However, when γ is closer to unity, the loss of growth factor by media flow can affect the cell culture. Also, even when γ is large, the convective losses might dominate the secretion rates at high Peclet numbers, and the growth factor concentration can drop considerably.

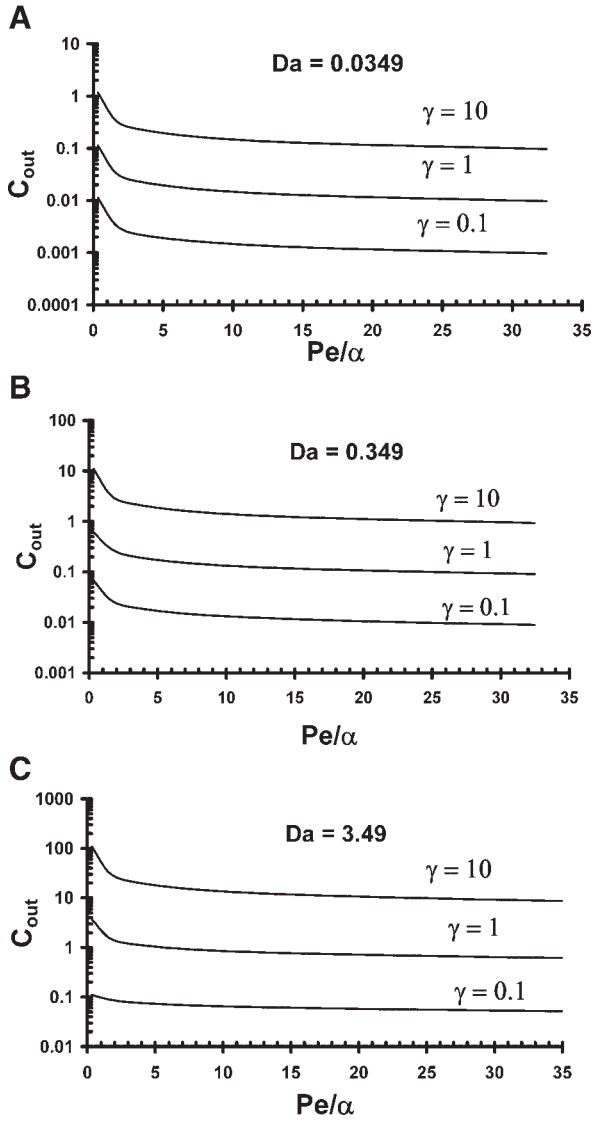

Figure 5. The dimensionless outlet concentration C_{out} of the cell secreted autocrine growth factor at the cell-media interface (at X = 1, Y = 1) as a function of the operating variable group Pe/α for various values of ratio γ and Da. The concentration variable is scaled by the uptake parameter $K_{m,gf}$, set at 1 nM. The base case parameters values (for Da = 0.349) are as per Table III. It can be seen that the dependence of dimensionless concentration of the autocrine growth factor on the value of Da is approximately linear for constant γ in the range of Pe/α described in the figure.

Figure 5 shows the effect of the operating variable group Pe/α on the outlet concentration of the cell secreted autocrine growth factor. As we increase the media flow, or change other parameters (see Table I) so as to increase the value of Pe/α, we are effectively pushing larger volumes of the media in the given time, thereby decreasing the concentration of the autocrine growth factor. This argument is valid irrespective of the value of γ or Da; however, the magnitude of the decrease depends on the values of γ and Da. Also, increasing the value of γ increases the rate of secretion compared to the uptake, and hence the outlet concentration of the growth factor increases as γ is increased. Similarly, an increase in the value of Da is indicative of an increased uptake/secretion rate compared to diffusive flux, and hence increased Da increases the outlet concentration of the growth factor.

The results can be interpreted in a slightly different manner by comparing the continuous culture experiment modeled here with a static culture protocol. For a static culture all of the growth factor is retained inside the media until the media is changed, typically every 2–3 days. For the continuous culture the media is continually replaced, and there is loss of the cell-secreted soluble growth factor through the media outflow. One way to compare these two protocols is by analyzing the fraction of autocrine growth factor lost. We can calculate the fraction of autocrine growth factor lost in the continuous culture experiment by dividing the integrated convective flux at the outlet to the total rate of production of the growth factor inside the reactor. Mathematically it is equivalent to the following equation

$$f = \frac{\left(\int_0^H u_x c_{gf}\,dy\right)}{\int_0^L \phi q_{gf}\,dx} \tag{16}$$

This is valid as we do not explicitly consider the degradation of growth factor in the model, and as per mass balance, the fraction retained inside the reactor is consumed by the cells, or in other words binds to the receptors and is functional.

Figure 6 shows the model results for the fraction of growth factor lost due to convective transport for different values of γ and Da. There is a significant loss of growth factor even for higher values of γ at the lower values of Da. Physically this implies that in the case of low density cell cultures, or with small molecules (greater diffusivity) which are loosely bound to the cell receptors, there is a high probability of the growth factor being lost in the media outflow. This result is especially relevant for the initial times during the cell culture, and hints that a strategy to retain the growth factors would be to start with a lower flow rate initially, and then increasing the flow as the cells proliferate inside the reactor.

DOI 10.1002/bit

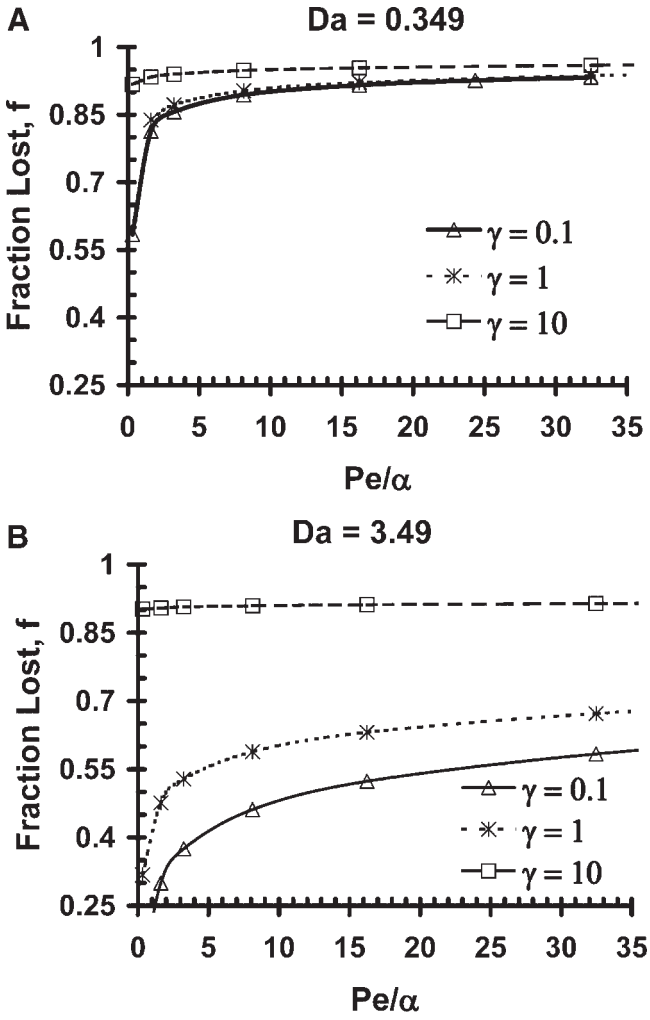

Figure 6. The fraction of the cell secreted autocrine growth factor lost as a function of the operating variable group Pe/α for various values of ratio γ and Da. The fraction is calculated from the results of the model using the relationship $f = (\int_0^H u_x c dy) \Big/ \int_0^L \phi q_{gf} dx$, where the numerator is evaluated at x = L, and denominator in the cell domain. q_{gf} is the rate of secretion of the growth factor. The fraction lost varies over a very small range (0.95–0.99) for values of Pe/α in the range 1.5–35 for Da = 0.0349 (not shown).

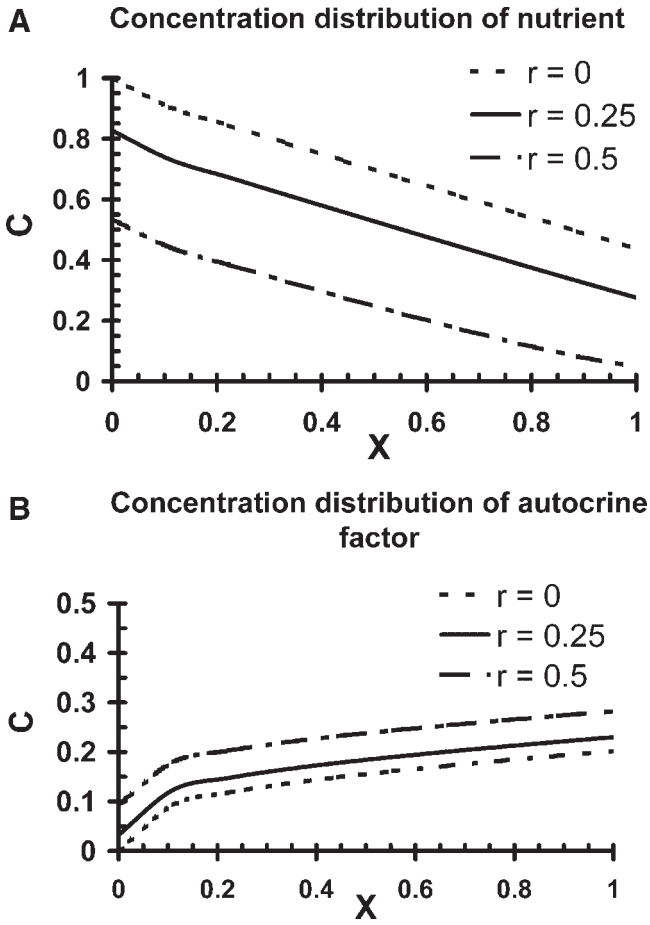

Figure 7. Effect of recirculation ratio r on the dimensionless concentration (C) of the autocrine growth (**a**) and nutrient concentration (**b**) along the dimensionless axial distance (X) at the cell media interface (Y = 1). The results are shown for the base case parameters for both the nutrient and the autocrine growth factor concentrations as per Table III.

Steady State Model Analysis at Constant Cell Density: Effect of Media Recirculation

One way to increase growth factor retention inside the bioreactor is to recycle a fraction of the outlet stream. For example, advances in the microfluidic Braille valve controls for microchannel reactors (Gu et al., 2004) can be used to design microchannels with flow recirculation. Such a system can be designed based on two possible schemes as shown in Figure 2. For most real systems the situation is much closer to the scheme (B). For recirculation scheme (A) the effective concentration of the growth factor inside the reactor would be a balance of the increasing effect brought about by recirculation and the decreasing effect due to the increased flow as per Figure 5. Alternatively, scheme (B) would tend to increase the concentration without any flow effect. Furthermore, model analysis of scheme (B) can give a clear understanding of the effect of recirculation without the confounding effects of a changing effective flow rate inside the reactor, and so we study the effect of recirculation as per scheme (B).

Figure 7a shows the effect of the recirculation ratio *r* on the axial distribution of the growth factor concentration at the cell-media interface for scheme (B) for the case of $\gamma = 1$. As expected, an increased recirculation ratio increases the concentration of the autocrine growth factor inside the reactor and also it is seen that the concentration of the autocrine growth factor builds up as we move downstream. However it should be considered that recycling the exit fluid will also mean that effective concentration of the nutrient in the bioreactor is lowered. Figure 7b shows the spatial distribution of the nutrient concentration for different recirculation ratios for same operating conditions. Clearly, the larger the recirculation ratio, the lower is the nutrient concentration inside the reactor. While we gain in terms of growth factor retention by recirculation, a key nutrient may be depleted. The choice of the fraction to recycle hence will have to be optimized for adequate retention of growth factor and also

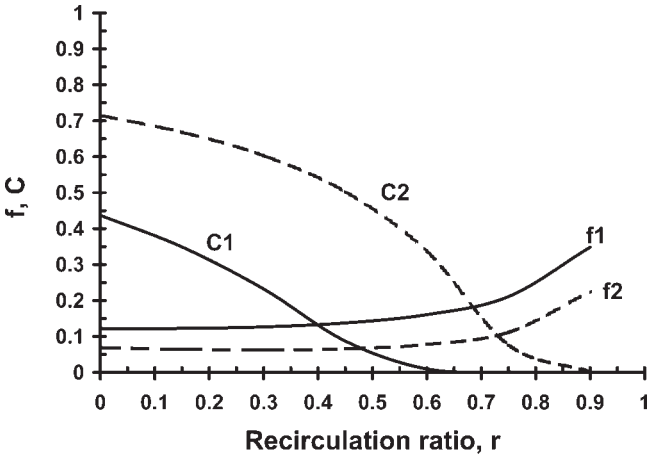

Figure 8. Optimization of the recirculation ratio for adequate growth factor retention and nutrient availability inside the reactor. The fraction of autocrine growth factor retained (f1, f2) and the non dimensional outlet concentration of the nutrient at the cell-media interface (C1, C2) are plotted as a function of the recirculation ratio. Results for two different values of Da based on the nutrient uptake rates are shown. Da = 0.105 corresponding to C1, f1 and Da = 0.0525 corresponding to C2, f2. The parameter γ is set to unity and other parameter values are as per Table III, while cell density value is changed to set the value of Da as indicated.

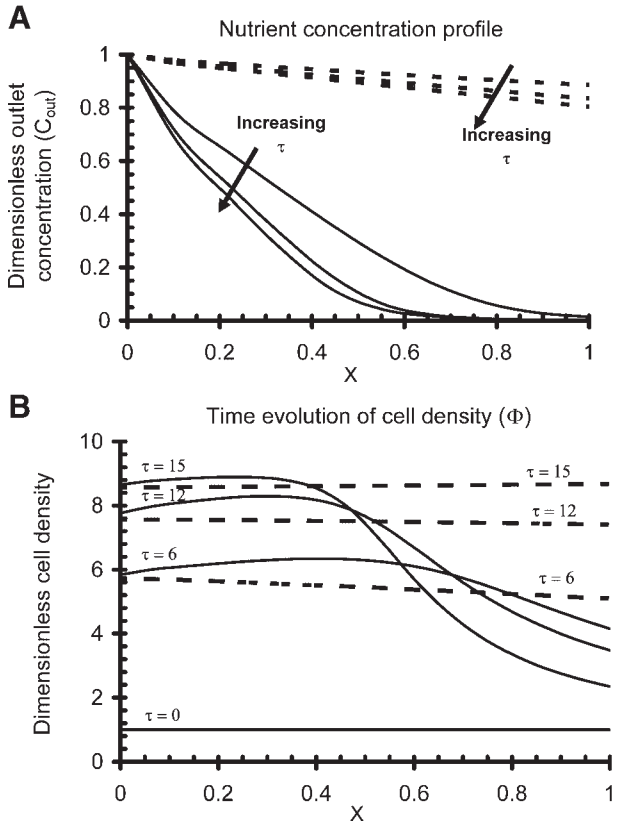

Figure 9. Effect of nutrient gradients on the cell density distribution inside the bioreactor. We show the impact of nutrient gradients using two example cases; case-1 (solid lines) with significant axial gradients, and case-2 (broken lines) with negligible depletion of the nutrient. The dimensionless concentration of nutrient at the cell-media interface along the non dimensional axial distance of the reactor is shown in figure (**a**), for various times ($\tau = 6$, 12, 15) for both the cases. **b** shows the time evolution of cell density as a function of the non dimensional axial distance of reactor. Initially the cell density is assumed to be uniform ($\Phi = 1$). Cell growth, reactor operation, and nutrient uptake parameters are as per Table III.

adequate nutrient availability. Figure 8 shows the effect of recirculation on both the growth factor retained inside the reactor and the nutrient outlet concentration for a conservative case of $\gamma = 1$ and a constant Pe/α. The optimal recirculation ratio can be determined by predefined thresholds of nutrient/growth factor concentrations that are required for functioning of the cells. Clearly when both the criteria are not met with one operating condition, it would be required to supplement the media with extra growth factor or nutrient. Furthermore, Figure 8 shows the effect of the Damkohler number on the location of the optimal recirculation ratio. Clearly with larger values of *Da*, the depletion of the nutrient is more significant, and so the optimal recirculation ratio would tend to be lower when operating at higher cell densities. Physically, it can be argued from the results that cell culture processes with larger cell density can be controlled more effectively with small amounts of recirculation for cases where the value of γ is close to unity.

Cell growth and differentiation is governed in large part by cell-secreted molecules; for example, the role of BMP in osteoblast differentiation is well known. Furthermore experiments with osteoblastic cell lines in microfluidic environment have revealed an effect of media flow rate on the cell growth and differentiation (Leclerc et al., 2006). Although the quantitative effect of growth factor washout cannot be interpreted from these experiments due to confounding processes like flow-associated cell washout, regulation of growth factor secretion and the limited number of flow rates tested, the results are qualitatively consistent with our predictions in Figure 6 and suggest that recirculation strategies might be implemented here to help efficiently cue the cells towards the desired behavior.

Unsteady State Model Analysis: Long Term Cell Proliferation

The long term performance of the bioreactor can be studied by understanding the cell response to the nutrient gradients inside the bioreactor. Figure 9 depicts the results of the solution of the coupled model with cell proliferation and the nutrient mass balance. The model results indicate that the nutrient gradients inside the bioreactor can affect the cell density distribution as cells proliferate inside the reactor. The higher concentration of the nutrient at the inlet favors rapid proliferation of the cells near upstream, which acts to deplete the nutrient and thus the nutrient concentration decreases along the axial dimension of the reactor. The cells downstream hence proliferate slowly, and in extreme cases can also suffer from starvation resulting in cell death. Clearly, then, gradients in nutrient concentration can limit the working volume of the reactor channel by selectively proliferating only upstream sections of the channel.

In agreement with our results, Gu et al. (2004) found that even when initially C2C12 cells are seeded uniformly

DOI 10.1002/bit

inside a channel, the cell density distribution evolves a dependence on the axial dimension, presumably in response to the gradients of nutrient concentrations inside the reactor. Using the information on cell characteristics and the model results as shown in Figure 3, one could design and operate the reactor to avoid cell density gradients in the reactor for such systems, for example by increasing the inlet concentration (decreasing *Da*) or increasing the flow rate (increasing Pe/α).

More interestingly, it may be desirable to have gradients of chemical signaling molecules inside the channel. For example, in applications involving tissue engineering of liver, the gradients of oxygen inside the reactor can simulate an in vitro model of zonation which is important in developing bio-artificial liver and also for studying drug metabolism in liver (Allen and Bhatia, 2003). In this scenario, the model could also be used to develop an operating strategy to ensure that all cells proliferate equally during the initial proliferation stage, while appropriate environments can be provided at a later stage of development by changing the operating conditions inside the reactor.

Effect of Cell Type Heterogeneity

Novel tissue engineering applications involve the co-culturing of different cell types to achieve a functional tissue or organ (e.g., Koller et al., 1997, for hematopoietic tissue). The introduction of different cell types inside the bioreactor can introduce several levels of complexities in the design and operation of the bioreactor in terms of sustained viability, growth, and function of all the cell types. We demonstrate the use of the model by considering the case of cell proliferation in a co-culture with two cell types with doubling times t_{d1} and t_{d2}, and we assume that there is a maximum carrying capacity of the reactor $(\Phi_1 + \Phi_2)_{max}$.

Both nutrient and spatial limitations govern the time evolution of the individual cell densities, and in general the composition of the cell co-culture will change over time. As shown in Figure 10 for the case of $t_{d1} = 16$ h and $t_{d2} = 32$ h, when the initial cell population is an equal mix of cell types 1 and 2 ($\Phi_2/\Phi_1 = 1$), the conditions favor the proliferation of cell type 1 and the cell population becomes largely of cell type 1 over time. Thus to achieve a long term co-culture of a specified composition, one must determine the appropriate initial mix to seed the reactor. The model can be used to calculate the initial cell densities of the individual cell type required to achieve the specified target composition at confluence. For example, in the case described above in Figure 10, if we want equal proportion of both cell types, starting with initial cell compositions of $\Phi_2/\Phi_1 \sim 5$, one can achieve a target composition of $\Phi_2/\Phi_1 \sim 1$. Although the full set of model equations must be solved to arrive at the plots shown in Figure 10, one can obtain a useful estimate of the required initial densities of cells to achieve a final target composition by considering spatial, but not nutrient, limitations in the reactor (Table II, case (e)). Indeed, assuming negligible cell death, we can simplify the ODEs

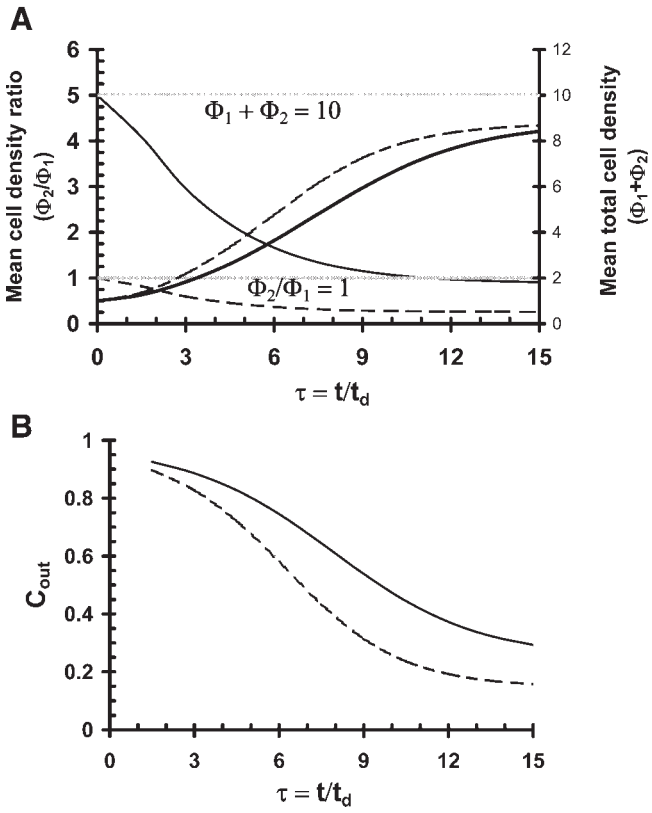

Figure 10. Effect of cell heterogeneity on the proliferation of cell co-culture of two cell types, with doubling times of $t_{d1} = 16$ and $t_{d2} = 32$ h and with dimensionless bioreactor carrying capacity $(\Phi_1 + \Phi_2)_{max} = 10$. (**a**) Both, the composition of the cell population represented by Φ_2/Φ_1 and the total cell density $(\Phi_2 + \Phi_1)$ are shown as a function of dimensionless time τ $(=t/t_{d1})$ for two different initial conditions. The cell density shown is averaged over the length of the reactor. Broken lines represent the dynamics of the culture starting at initial composition of by $\Phi_2/\Phi 1 = 1$, which also is the target composition (shown as the line $\Phi_2/\Phi_1 = 1$ in the figure). Solid lines are model results starting with an initial composition as estimated by model based on the doubling times. $(\Phi_2 = 0.15,\ \Phi_1 = 0.85)$. (**b**) Dimensionless outlet concentration of the nutrient species at the cell-media interface for both the initial conditions. The maximum carrying capacity of the reactor by space considerations is 10 times the initial cell density and signifies confluence shown as the line $\Phi_1 + \Phi_2 = 10$ in the figure. The uptake parameters for the two cell types are $V_{max,1} = 1.9e\text{-}16$ mol/s/cell, $V_{max,2} = 9.5$ e-17 mol/s/cell. The other parameters are as per Table III.

to arrive at the following relationship between the cell densities of the two types.

$$\frac{d\Phi_1}{d\Phi_2} = a\frac{\Phi_1}{\Phi_2} \tag{17}$$

where a is the ratio of the doubling times of the two cells types given by t_{d2}/t_{d1}. We have used the fact that the growth rate in the exponential regime follows the simple relationship $\mu_{g,max} = \ln(2)/t_d$.

Equation (17) can be used to estimate the initial composition required to achieve a target final composition in a simple manner. For the present case, we can back calculate the initial conditions required to achieve the final

target composition ($\sim \Phi_1 = \Phi_2 = 5$) for the given value of parameter a (=2) which gives the value of $\Phi_{1,0} = 0.15$, and $\Phi_{2,0} = 0.85$ resulting in the ratio $(\Phi_2/\Phi_1)_{\tau=0} = 5.67$. Hence, it can be seen that even in the presence of the nutrient gradients (Fig. 10b), the estimate from the ODE model using the analysis described above remains reasonable.

The ability to maintain a composition of cells in proliferating cell cultures can prove to be crucial in some important tissue engineering applications for example in culturing primary cells consisting of adult stem cells (Koller et al., 1997). Primary cells are inherently heterogeneous and adult stem cells form a very small percentage (<0.001%) of the cell population. The survival and controlled differentiation of these stem cells may require the presence of multiple cell types in a reactor. Model based analysis as described here can help to understand and overcome some of the problems encountered in such culture processes.

CONCLUSIONS

Microchannel reactors for tissue engineering are associated with a vast and largely uncharacterized design space and the design and operation of these bioreactors can be aided by mathematical modeling. We present here a coupled model for nutrient/growth factor distribution and cell proliferation in the microchannel bioreactor and use it to show how operating parameters (e.g., flow rate, recirculation) and design parameters (e.g., channel geometry, inoculum composition) can influence the cell growth in the bioreactor. We believe that models formulated on the basis of known qualitative or quantitative information on the systems of interest can be used to narrow the experimental design space, and can help in design and optimization of the bioreactors along with offering an insight into the fundamental functioning of such systems.

We thank D. Mooney, S. Takayama, W. Gu, N. Futai, and G Mehta for helpful discussions.

References

Allen JW, Bhatia SN. 2003. Formation of steady-state oxygen gradients in vitro. Biotechnol Bioeng 82(3):253–262.

Allen JW, Khetani SR, Bhatia SN. 2005. In vitro zonation and toxicity in a hepatocyte bioreactor. Toxicol Sci 84(1):110–119.

Andersson H, van den Berg A. 2004. Microfabrication and microfluidics for tissue engineering: State of the art and future opportunities. Lab Chip 4(2):98–103.

Ben-Abraham R, Gazit V, Vofsi O, Ben-Shlomo I, Reznick AZ, Katz Y. 2003. Beta-phenylpyruvate and glucose uptake in isolated mouse soleus muscle and cultured C2C12 muscle cells. J Cell Biochem 90(5):957–963.

Bhalla US, Iyengar R. 1999. Emergent properties of networks of biological signaling pathways. Science 283:381–387.

Botchwey EA, Dupree MA, Pollack SR, Levine EM, Laurencin CT. 2003. Tissue engineered bone: Measurement of nutrient transport in three-dimensional matrices. J Biomed Mater Res 67A(1):357–367.

da Silva CL, Goncalves R, Lemos F, Lemos MA, Zanjani ED, Almeida-Porada G, Cabral JM. 2003. Modelling of ex vivo expansion/maintenance of hematopoietic stem cells. Bioprocess Biosyst Eng 25(6):365–369.

Galban CJ, Locke BR. 1999. Effects of spatial variation of cells and nutrient and product concentrations coupled with product inhibition on cell growth in a polymer scaffold. Biotechnol Bioeng 64(6):633–643.

Ghanem A, Shuler ML. 2000. Characterization of a perfusion reactor utilizing mammalian cells on microcarrier beads. Biotechnol Prog 16(3):471–479.

Gu W, Zhu X, Futai N, Cho BS, Takayama S. 2004. Computerized microfluidic cell culture using elastomeric channels and Braille displays. Proc Natl Acad Sci USA 101(45):15861–15866.

Guarino RD, Dike LE, Haq TA, Rowley JA, Pitner JB, Timmins MR. 2004. Method for determining oxygen consumption rates of static cultures from microplate measurements of pericellular dissolved oxygen concentration. Biotechnol Bioeng 86(7):775–787.

Horner M, Miller WM, Ottino JM, Papoutsakis ET. 1998. Transport in a Grooved Perfusion Flat-Bed Bioreactor for Cell Therapy Applications. Biotechnol Prog 14:689–698.

Jorjani P, Ozturk SS. 1999. Effects of cell density and temperature on oxygen consumption rate for different mammalian cell lines. Biotechnol Bioeng 64(3):349–356.

Koller MR, Emerson SG, Palsson BO. 1993. Large-scale expansion of human stem and progenitor cells from bone marrow mononuclear cells in continuous perfusion cultures. Blood 82(2):378–384.

Koller MR, Manchel I, Palsson BO. 1997. Importance of parenchymal:stromal cell ratio for the ex vivo reconstitution of human hematopoiesis. Stem Cells 15(4):305–313.

Lauffenburger D, Cozens C. 1989. Regulation of mammalian cell growth by autocrine growth factors: Analysis of consequences for inoculum cell density effects. Biotechnol Bioeng 33(11):1365–1378.

Lauffenburger DA, Linderman JJ. 1993. Receptors: Models for binding, trafficking, and signalling. Oxford: Oxford University Press.

Leclerc E, Sakai Y, Fujii T. 2003. Cell culture in 3-dimensional microfluidic structure of PDMS (polydimethylsiloxane). Biomedical Microdevices 5(2):109–114.

Leclerc E, Sakai Y, Fujii T. 2004. Microfluidic PDMS (polydimethylsiloxane) bioreactor for large-scale culture of hepatocytes. Biotechnol Prog 20(3):750–755.

Leclerc E, David B, Griscom L, Lepioufle B, Fujii T, Layrolle P, Legallaisa C. 2006. Study of osteoblastic cells in a microfluidic environment. Biomaterials 27(4):586–595.

Locker M, Kellermann O, Boucquey M, Khun H, Huerre M, Poliard A. 2004. Paracrine and autocrine signals promoting full chondrogenic differentiation of a mesoblastic cell line. J Bone Miner Res 19(1):100–110.

Netti PAFT, Jain RK. 2003. Coupled macromolecular transport and gel mechanics: Poroviscoelastic approach. AIChE J 49(6):1580–1596.

Obradovic B, Meldon JH, Freed LE, Vunjak-Novakovic F. 2000. Glycosaminoglycan deposition in Engineered Cartilage: Experiments and Mathematical Model. AIChE J 46(9):1860–1871.

Oehrtman GT, Wiley HS, Lauffenburger DA. 1998. Escape of autocrine ligands into extracellular medium: Experimental test of theoretical model predictions. Biotechnol Bioeng 57(5):571–582.

Pathi P, Ma T, Locke BR. 2005. Role of nutrient supply on cell growth in bioreactor design for tissue engineering of hematopoietic cells. Biotechnol Bioeng 89(7):743–758.

Rawadi G, Vayssiere B, Dunn F, Baron R, Roman-Roman S. 2003. BMP-2 controls alkaline phosphatase expression and osteoblast mineralization by a Wnt autocrine loop. J Bone Miner Res 18(10):1842–1853.

Roy P, Baskaran H, Tilles AW, Yarmush ML, Toner M. 2001. Analysis of oxygen transport to hepatocytes in a flat-plate microchannel bioreactor. Ann Biomed Eng 29(11):947–955.

DOI 10.1002/bit

Shvartsman SY, Wiley HS, Deen WM, Lauffenburger DA. 2001. Spatial range of autocrine signaling: Modeling and computational analysis. Biophys J 81(4):1854–1867.

Wiley HS, Shvartsman SY, Lauffenburger DA. 2003. Computational modeling of the EGF-receptor system: A paradigm for systems biology. Trends Cell Biol 13(1):43–50.

Williams KA, Saini S, Wick TM. 2002. Computational fluid dynamics modeling of steady-state momentum and mass transport in a bioreactor for cartilage tissue engineering. Biotechnol Prog 18:951–963.

Zandstra PW, Conneally E, Petzer AL, Piret JM, Eaves CJ. 1997. Cytokine manipulation of primitive human hematopoietic cell self-renewal. Proc Natl Acad Sci USA 94(9):4698–4703.